nature portfolio

https://doi.org/10.1038/s41563-022-01360-9

Supplementary information

Nanoparticle-modified microrobots for in vivo antibiotic delivery to treat acute bacterial pneumonia

In the format provided by the authors and unedited

Nanoparticle-modified microrobots for in vivo antibiotic delivery to treat acute bacterial pneumonia

Fangyu Zhang[1†], Jia Zhuang[1†], Zhengxing Li[1†], Hua Gong[1†], Berta Esteban-Fernández de Ávila[1], Yaou Duan[1], Qiangzhe Zhang[1], Jiarong Zhou[1], Lu Yin[1], Emil Karshalev[1], Weiwei Gao[1], Victor Nizet[2], Ronnie H. Fang[1], Liangfang Zhang[1*] and Joseph Wang[1*]

[1] Department of NanoEngineering and Chemical Engineering Program, University of California San Diego, La Jolla, CA 92093, United States.

[2] Department of Pediatrics and Skaggs School of Pharmacy and Pharmaceutical Sciences, University of California San Diego, La Jolla, CA 92093, United States.

[†]These authors contributed equally to this work.

[*]E-mail: josephwang@ucsd.edu; zhang@ucsd.edu

Table of contents:

Supplementary Figures

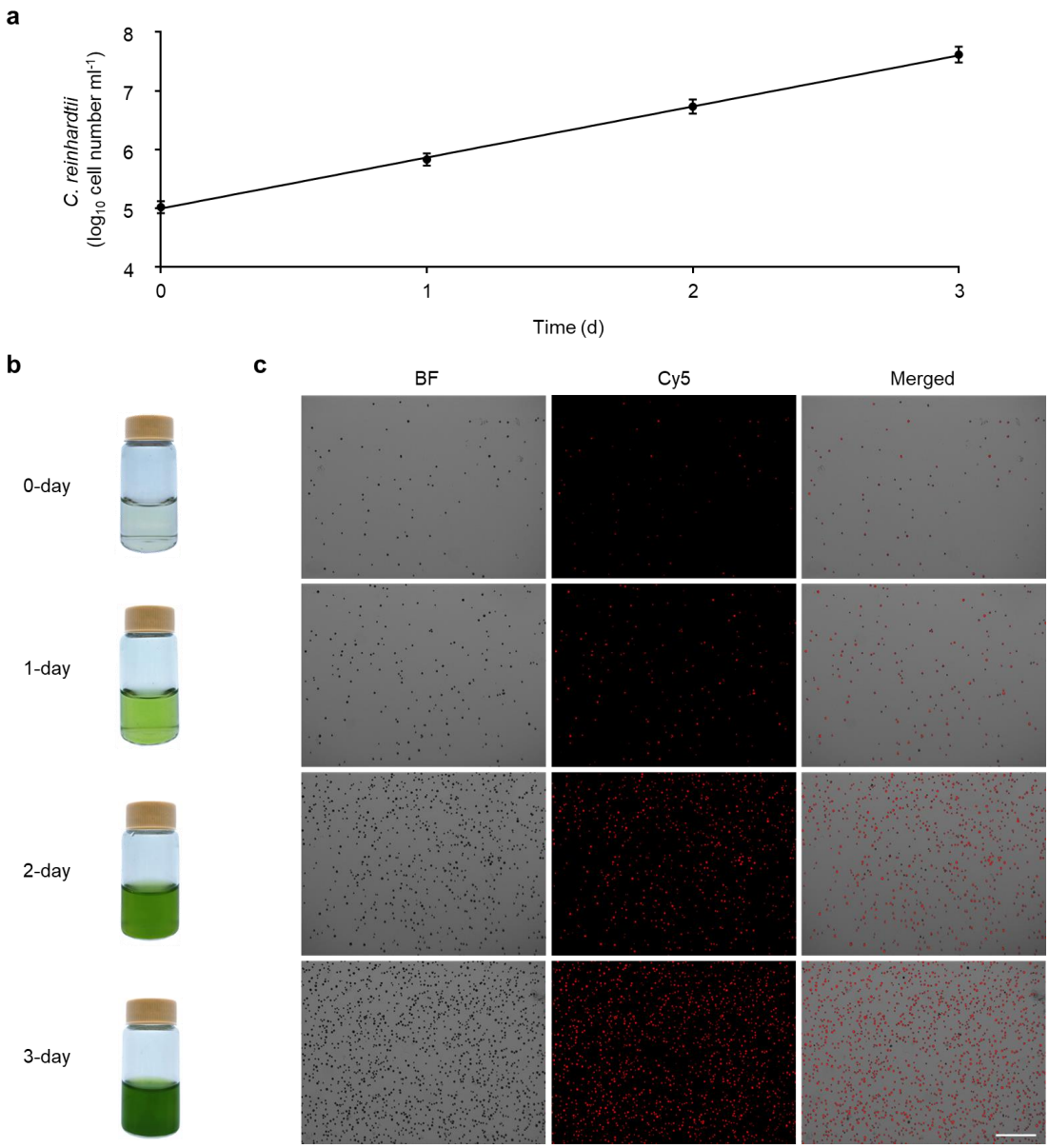

Supplementary Figure 1. *C. reinhardtii* algae cultured at optimal conditions in TAP medium. a, Algae growth curve over 3 days at optimal conditions in TAP medium (n = 3; geometric mean ± s.d.). **b,** Photographs of the algae growth for 3 days. **c,** Brightfield, fluorescence, and merged microscopy images of algae taken during a 3-day culture period. Scale bar: 200 μm. Independent experiments (n = 3) were performed with similar results.

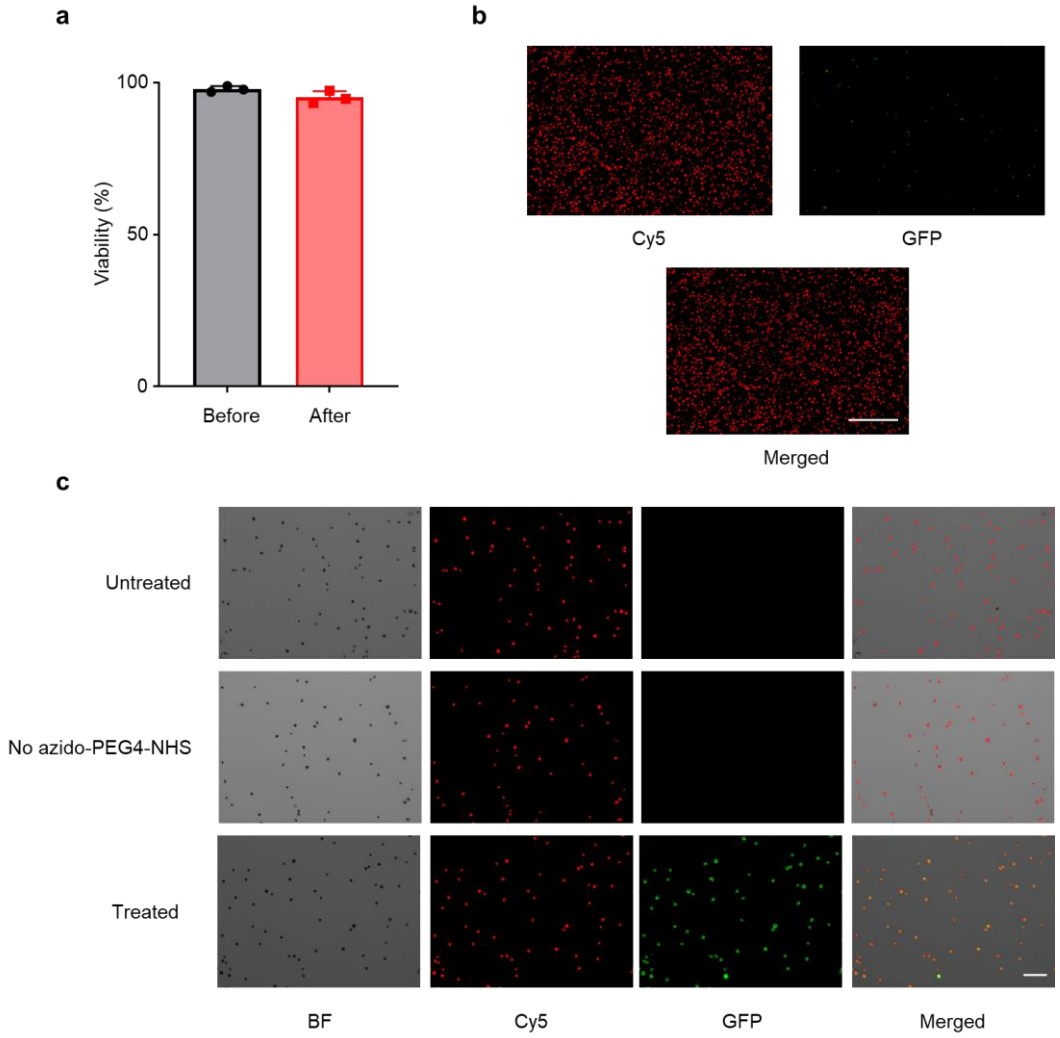

Supplementary Figure 2. Cytotoxicity evaluation of azido-PEG$_4$-NHS ester on the algae and further confirmation of azido groups modification on the algae. a, Viability study of algae before and after azido-PEG$_4$-NHS ester modification (n = 3; mean + s.d.). **b,** Microscopy images of live and dead algae after azido-PEG4-NHS ester modification. Red channel: autofluorescence of live algae; green channel: SYTOX labeled dead algae. Scale bar: 400 μm. **c,** Representative microscopy images of untreated algae, unmodified algae with DBCO-based fluorescence probe, and azido-PEG4-NHS ester-modified algae labeled with a DBCO-based fluorescence probe. Red channel: autofluorescence of algae; green channel: azide-modified algae with BDP FL DBCO probe. Scale bar: 100 μm. In panels b and c, independent experiments (n = 3) were performed with similar results.

Results: Viability tests demonstrated that such reaction conditions resulted in negligible cytotoxicity to the algae (Supplementary Fig. 2a), and this was also confirmed by a SYTOX fluorescence assay[1] (Supplementary Fig. 2b). The presence of azido groups on the surface of the algae was determined by covalently binding a DBCO-based fluorescence probe. Fluorescent imaging confirmed the successful modification of azido groups onto the algae (Supplementary Fig. 2c).

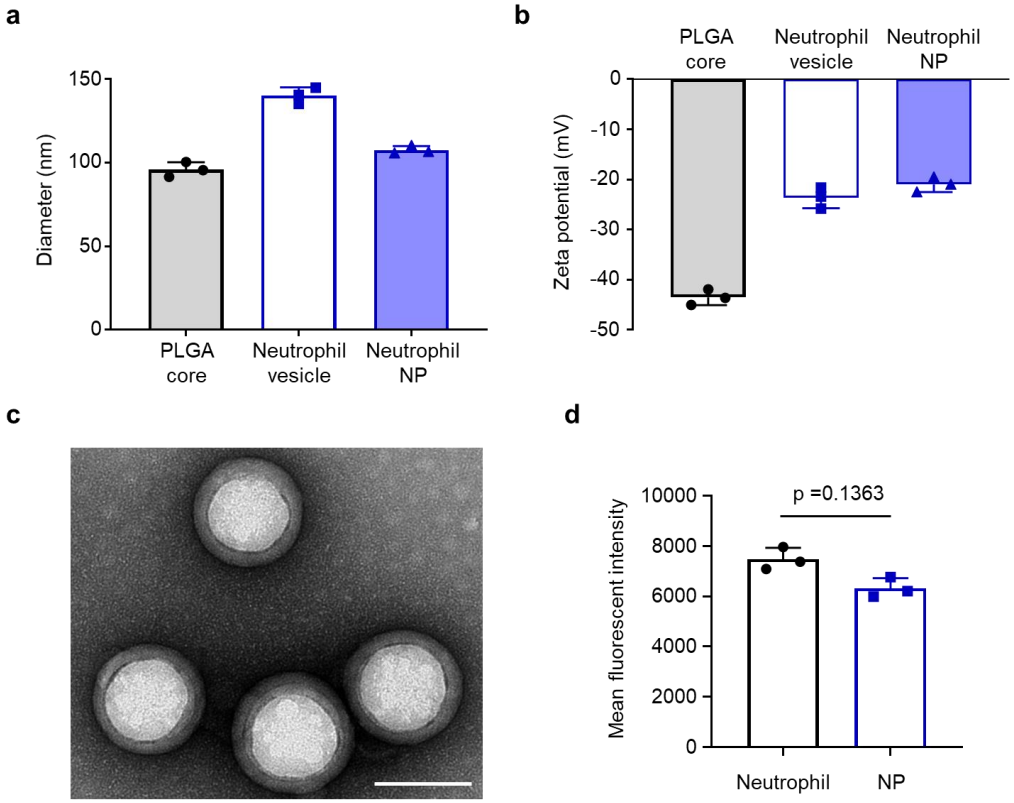

Supplementary Figure 3. Characterization of neutrophil membrane coated nanoparticles (NP). a,b, Hydrodynamic size (diameter) (a) and surface zeta potential (b) of PLGA cores, neutrophil vesicles, and neutrophil membrane coated nanoparticles measured by dynamic light scattering (DLS) (n = 3; mean + s.d.). **c,** Representative TEM image of neutrophil membrane coated nanoparticles. Scale bar: 100 nm. Independent experiments (n = 3) were performed with similar results. **d,** Comparison of the fluorescence intensity measured in neutrophils (~2.5 × 10^6 cells) and neutrophil membrane-coated PLGA nanoparticles (NP) (100 µl, 0.5 mg ml^{-1} protein content) containing equal amounts of membrane content and stained with Alexa488 anti-human CD11a (LFA-1) antibody (n = 3; mean + s.d.). ns: not significant; Student's two-tailed *t*-test for d.

Results: PLGA cores were first prepared following a double emulsion solvent evaporation method[2]. To synthesize neutrophil membrane-coated PLGA nanoparticles (denoted 'NP'), plasma membrane derived from human HL-60 cells was coated onto PLGA cores and confirmed by size (Supplementary Fig. 3a) and surface zeta potential measurements (Supplementary Fig. 3b) using dynamic light scattering (DLS). The integrity of the core-shell structure of the resulting NP was also visualized by transmission electron microscopy (TEM) (Supplementary Fig. 3c). A right-side-out membrane orientation was verified by immunostaining, quantifying LFA-1 antigen on NP and comparing it with that on neutrophil cells with an equal amount of membrane proteins (Supplementary Fig. 3d). The NP group showed a comparable fluorescence intensity with that of the neutrophil group, indicating that the right-side-out membrane orientation was achieved during the NP fabrication process, which is consistent with what has been reported before[3].

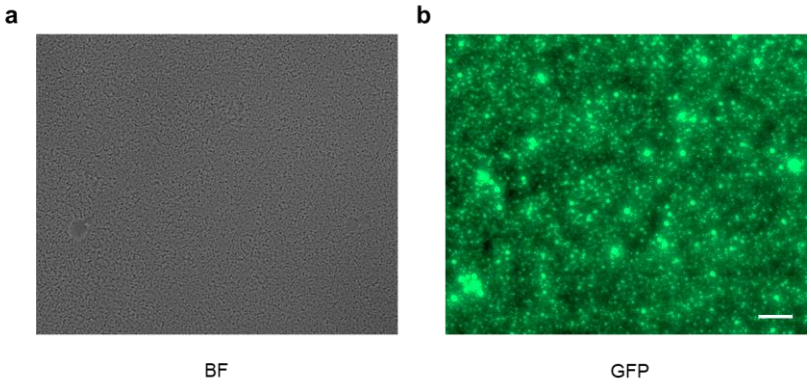

Supplementary Figure 4. Confirmation of DBCO-PEG$_4$-NHS ester conjugation to NPs. a,b, Representative microscopy brightfield (a) and fluorescence (b) images of NP incubated for 1 h with DBCO-PEG$_4$-NHS ester and labeled with an azido-based fluorescence probe. Scale bar: 1 μm. Independent experiments (n = 3) were performed with similar results.

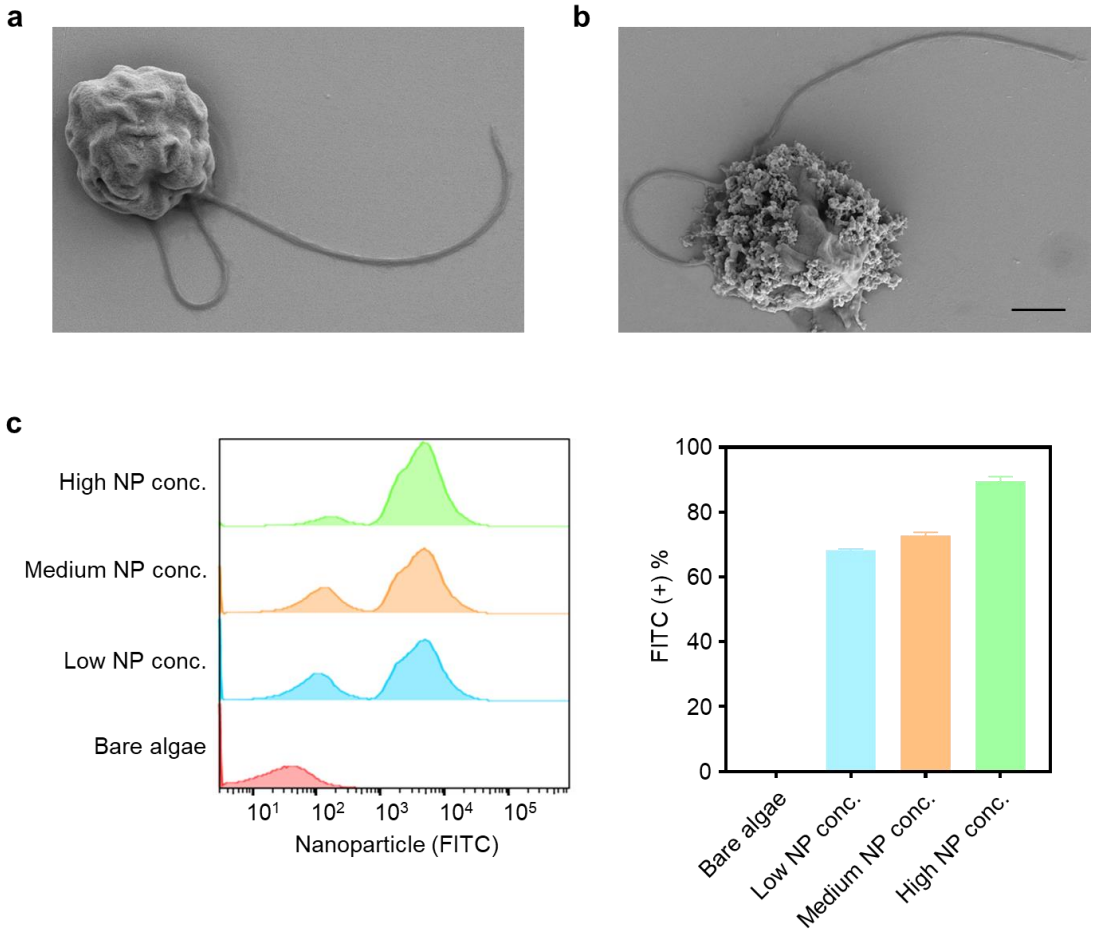

Supplementary Figure 5. Characterization of the morphology and optimization of NP binding efficiency of algae-NP-robot. a,b, SEM images of bare algae (a) and algae-NP-robot (b). Scale bar: 2 μm Independent experiments (n = 3) were performed with similar results. **c,** Representative flow cytometry analysis of algae modified with NP at various NP concentrations.

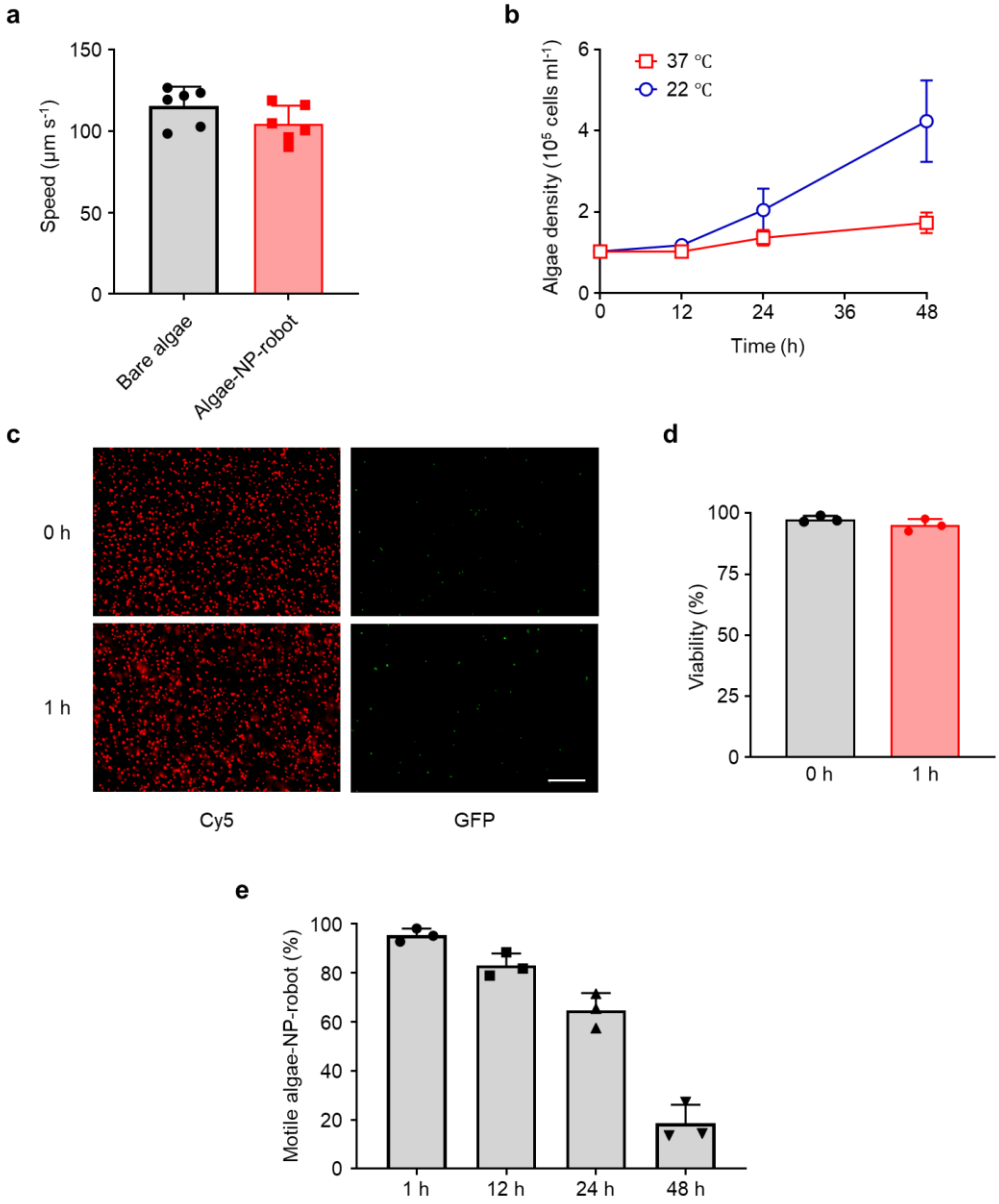

Supplementary Figure 6. **Motion and physiological properties of bare algae and algae-NP-robot in different media. a,** Motion performance of bare algae and algae-NP-robot in TAP medium at room temperature (n = 6; mean + s.d.). **b,** Growth curve of bare algae in simulated lung fluid (SLF) at room temperature and body temperature (n = 3; mean + s.d.). **c,d,** Representative microscopy fluorescence images (c) and viability (d) of algae-NP-robot before and after 1 h of motion in SLF (n = 3; mean + s.d.). Red channel: autofluorescence of live algae; green channel: SYTOX labeled dead algae. Scale bar: 200 μm. **e,** Percentage of motile algae-NP-robot after 1 h, 12 h, 24 h, and 48 h exposures to the SLF in the dark at body temperature (n = 3; mean + s.d.).

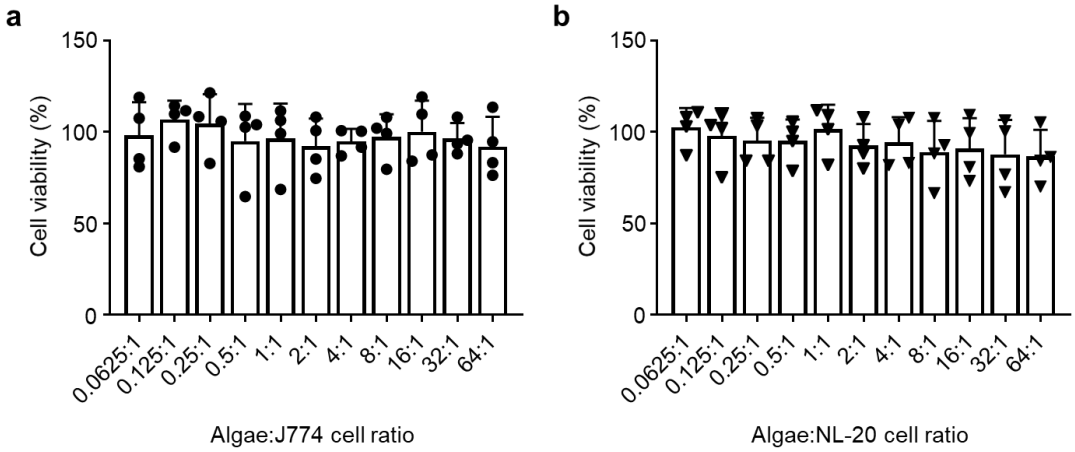

Supplementary Figure 7. Cytotoxicity of algae-NP-robot. a,b, Algae-NP-robot was incubated with J774 macrophages (a) and NL20 human lung epithelial cells (b), and cell viability was evaluated after 24 hours using a CellTiter Aqueous One Solution cell proliferation assay (n = 4; mean + s.d.).

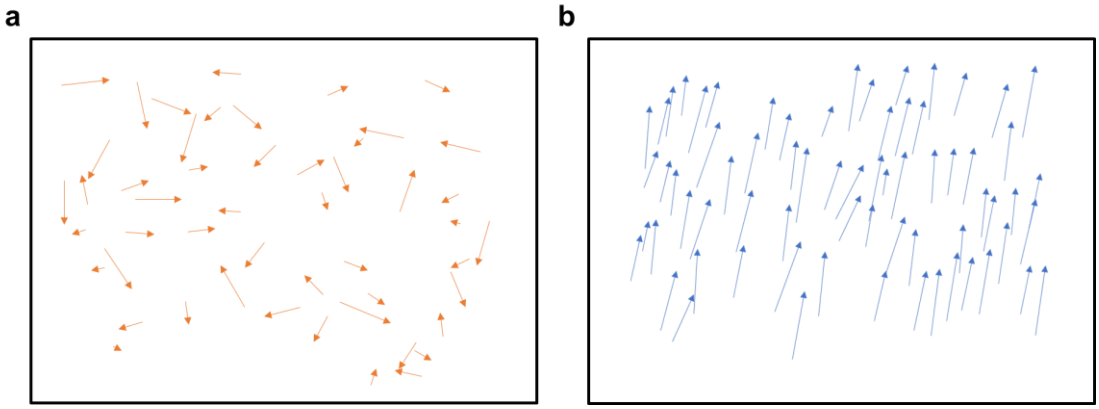

Supplementary Figure 8. **Comparison of the algae-NP-robot motion without (a) and with (b) an external light source.** The algae-NP-robot displayed random motion without the light, while showing a phototaxis motion towards the light when it was illuminated from the top. The arrows show the motion direction of algae-NP-robot during a 2 s interval.

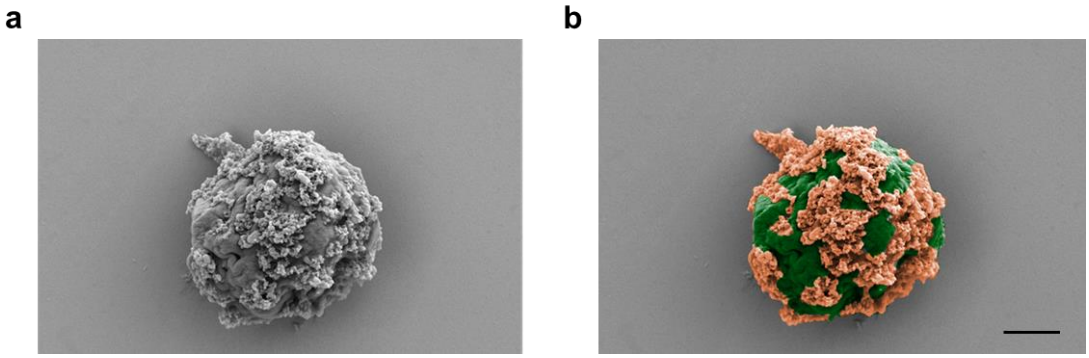

Supplementary Figure 9. Morphology of static algae-NP. a,b, SEM (a) and pseudocolored SEM (b) images of static algae-NP (without flagella). Scale bar: 2 μm. Independent experiments (n = 3) were performed with similar results.

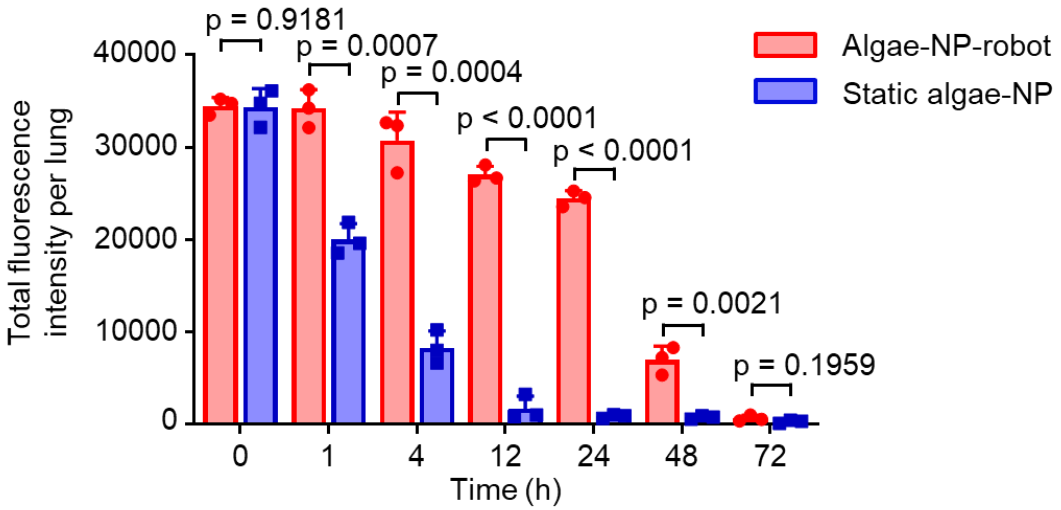

Supplementary Figure 10. Total fluorescence intensity per organ of lung samples from algae-NP-robot and static algae-NP treatment (n = 3; mean + s.d.). Student's two-tailed *t*-test.

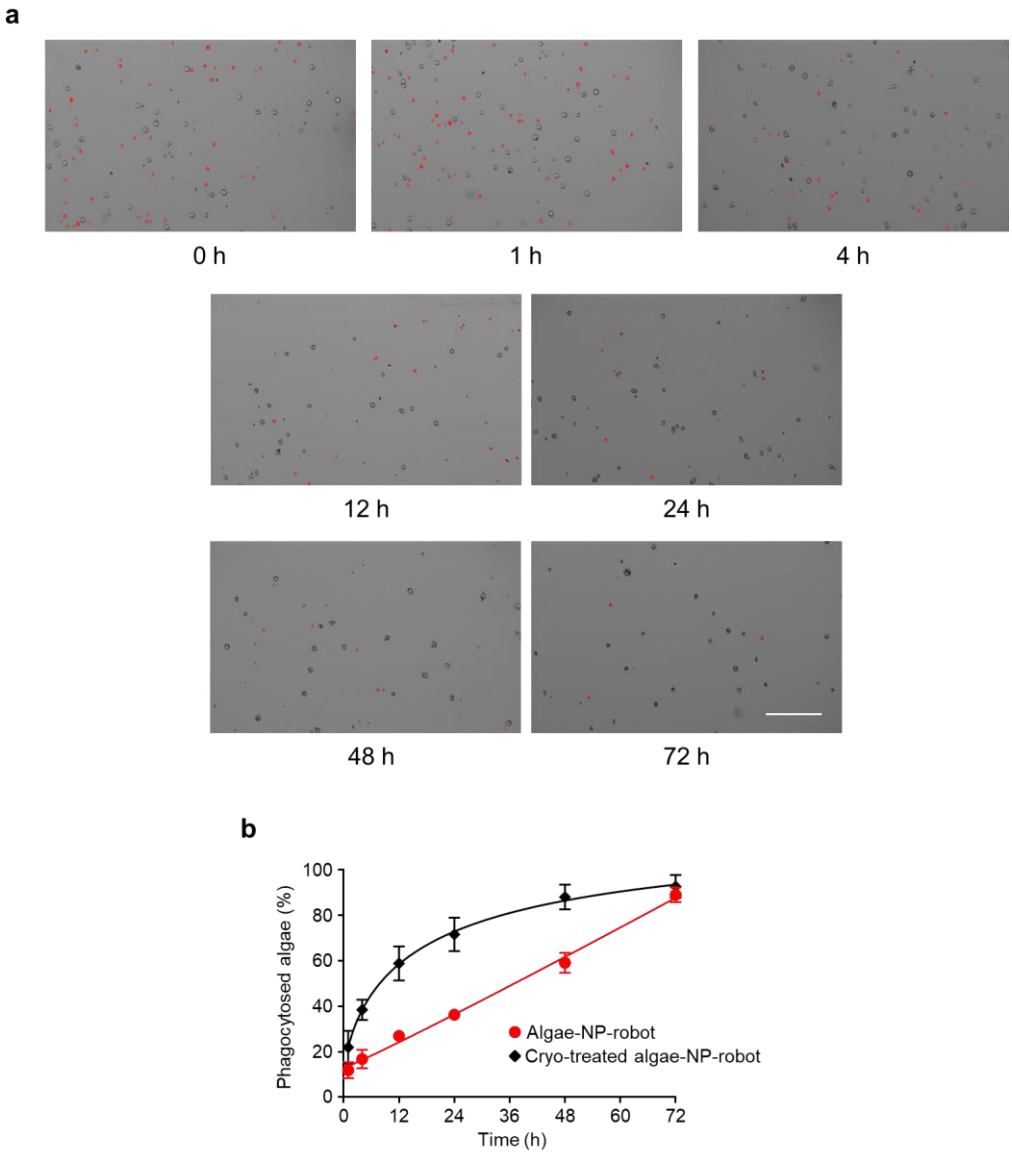

Supplementary Figure 11. In vitro uptake of algae-NP-robot by J774 macrophage. a, Representative microscopy images of algae-NP-robot incubated with J774 macrophages over the course of 72 h. Scale bar: 200 μm. **b,** Macrophage phagocytosis of algae-NP-robot or cryo-treated algae-NP-robot over time (n = 4; mean ± s.d.).

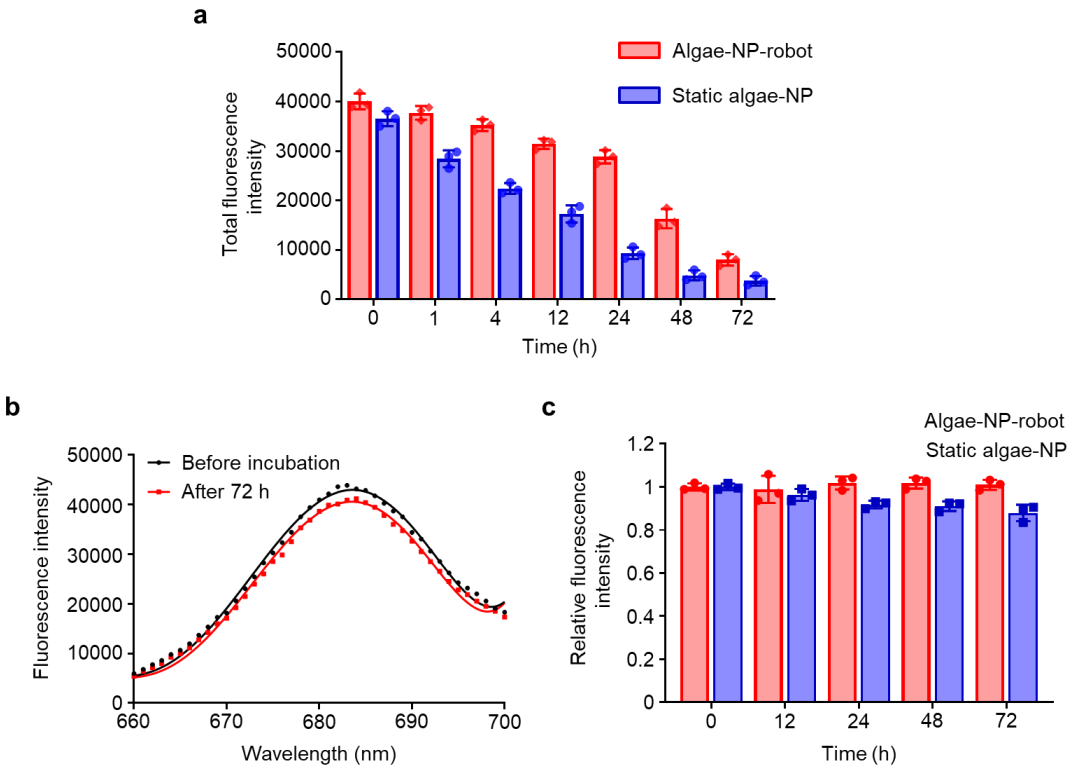

Supplementary Figure 12. Influence of the J774 macrophages uptake on the fluorescence of algae-NP-robot in vitro. a, Total fluorescence intensity of algae-NP-robot and static algae-NP incubated with J774 macrophages over the course of 72 h (n = 3; mean + s.d.). **b,** Optical spectra of algae-NP-robot before and after 72 h of incubation in cell culture medium without J774 macrophages at body temperature. **c,** Relative fluorescence intensity of algae-NP-robot and static algae-NP in cell culture medium without J774 macrophages during 72 h of incubation at body temperature (n = 3; mean + s.d.).

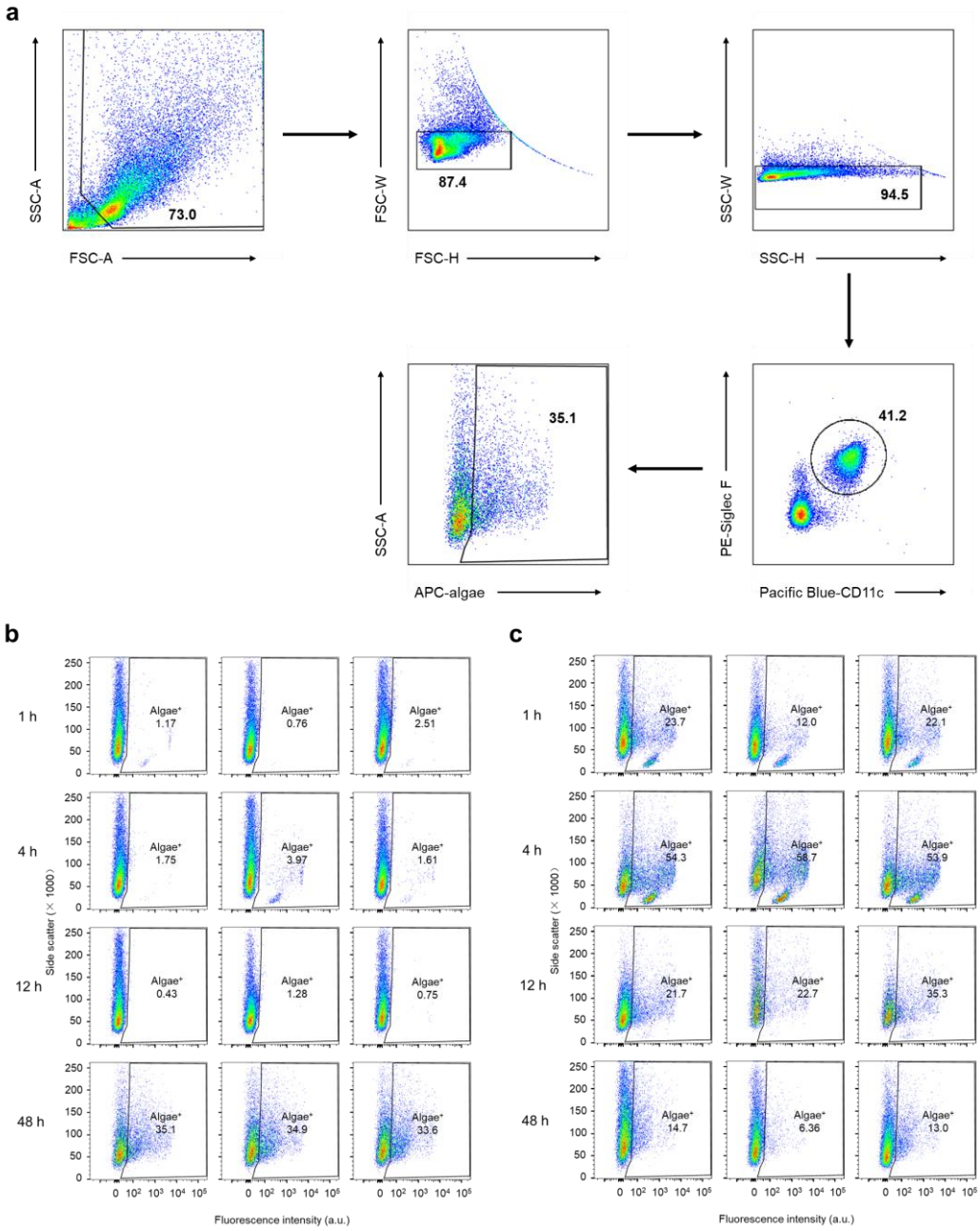

Supplementary Figure 13. Flow cytometry analysis of the uptake of algae-NP-robot and static algae-NP by alveolar macrophages. a, Gating strategy for quantitation of macrophage ($CD11c^+$ $Siglec\text{-}F^+$) uptake of algae-NP-robot and static algae-NP. **b,c,** Flow cytometric analysis of the uptake of algae-NP-robot (b) and static algae-NP (c) by alveolar macrophage at various timepoints (1 h, 4 h, 12 h, and 48 h) after intratracheal administration.

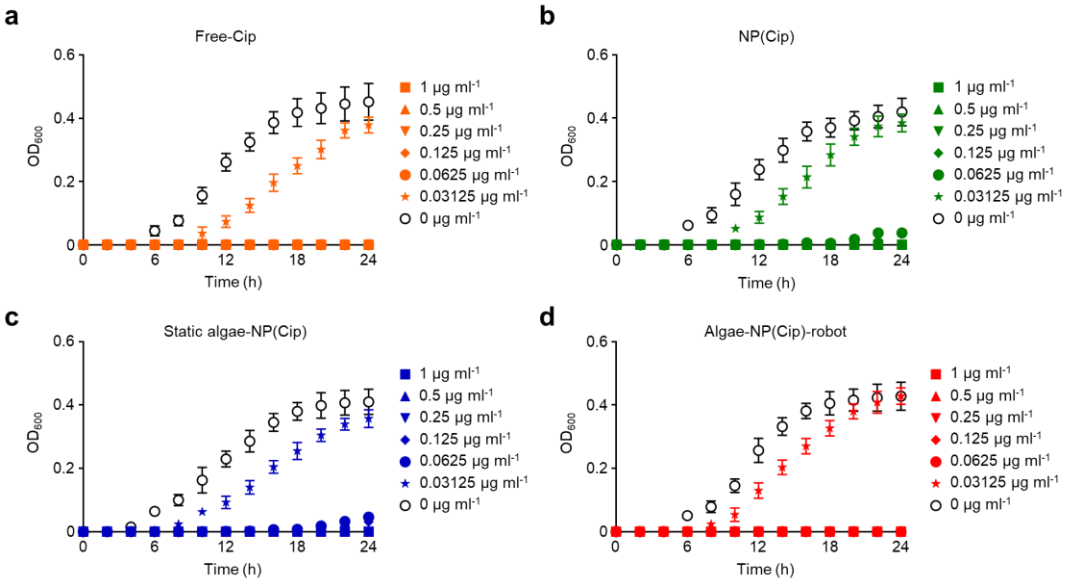

Supplementary Figure 14. Growth curve of *P. aeruginosa* with different concentrations of ciprofloxacin. a-d, OD_{600} of *P. aeruginosa* incubated with (a) free Cip , (b) NP(Cip), (c) static algae-NP(Cip), and (d) algae-NP(Cip)-robot at various Cip concentrations (n = 3; mean + s.d.).

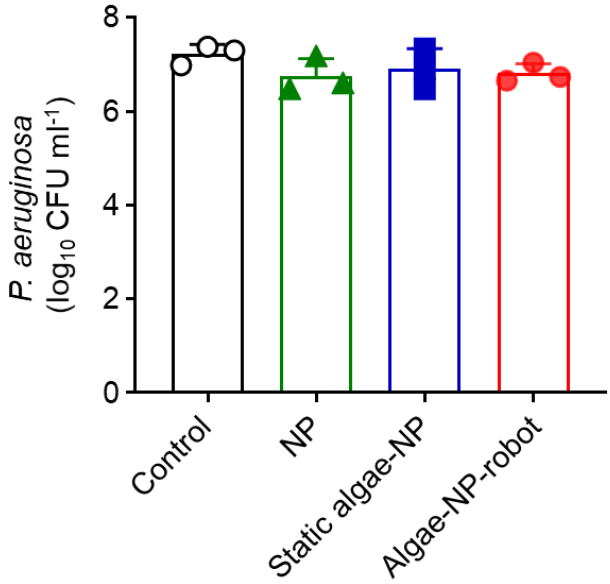

Supplementary Figure 15. Influence of NP and algae on the growth of *P. aeruginosa.* Bacterial enumeration of *P. aeruginosa* after 24 h of incubation with buffer, NP, static algae-NP, and algae-NP-robot (n = 3; geometric mean + s.d.).

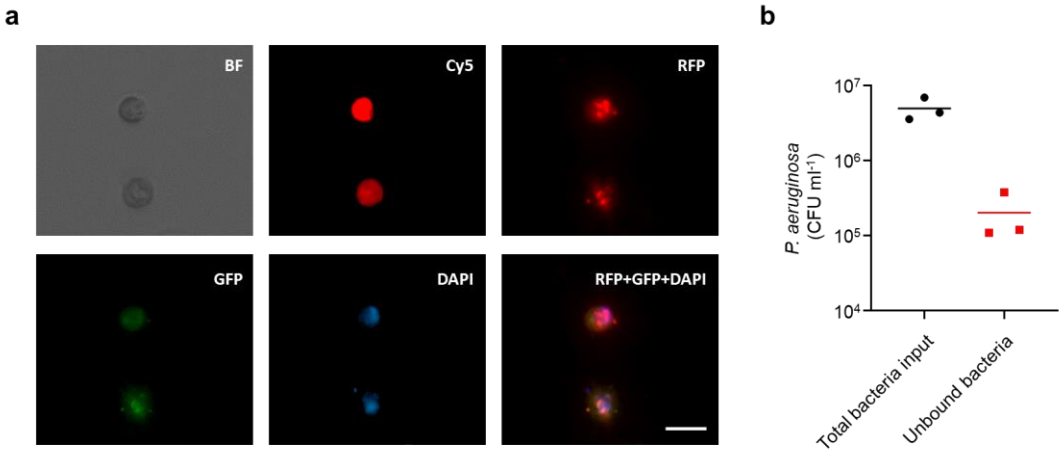

Supplementary Figure 16. **Binding between algae-NP-robot and *P. aeruginosa*. a,** Brightfield and fluorescent images of the binding of algae-NP-robot and *P. aeruginosa*. Autofluorescence of natural algae chloroplast in the Cy5 channel; DiO-labeled PLGA cores in the GFP channel; DiI-labeled cell membranes in the RFP channel; Hoechst 33342-labeled DNA of *P. aeruginosa* in the DAPI channel. Scale bar: 10 μm. Independent experiments (n = 3) were performed with similar results. **b,** Quantification of the binding efficiency between algae-NP-robot and *P. aeruginosa* by enumeration of colony forming units (CFU) of total bacteria input and unbound bacteria.

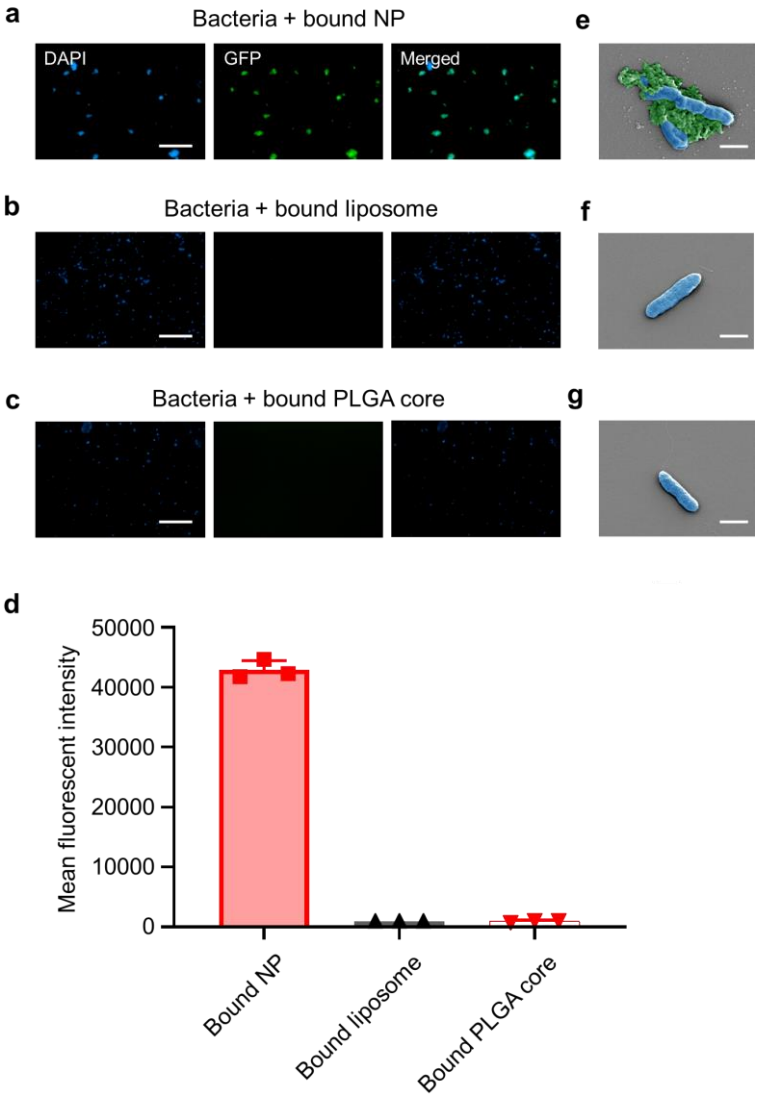

Supplementary Figure 17. Comparison of the binding of *P. aeruginosa* to neutrophil membrane-coated PLGA nanoparticles ('NPs'), liposomes, and PLGA nanoparticle cores without neutrophil membrane coating. a-c, Fluorescence microscopy demonstrating the binding ability of NPs (a), liposomes (b), and PLGA nanoparticle cores (c) with *P. aeruginosa* bacteria after washing away the unbound nanoparticles. DAPI channel: Hoechst 33342-labeled bacteria; GFP channel: Bound NPs, liposomes, or PLGA nanoparticle cores with DiO labeling. Scale bar: 50 μm. Independent experiments (n = 3) were performed with similar results. **d,** Quantification of bound NPs, liposomes, and PLGA nanoparticle cores on bacteria by measurement of the fluorescence intensity of DiO-labeled nanoparticles (λex/λem = 484 nm/501 nm; n = 3; mean + s.d.). **e-g,** Pseudocolored SEM images of NP (e), liposome (f) and PLGA core (g) binding to bacteria. Scale bar: 1 μm. The NPs can bind to bacteria (a, e) and induce aggregation of bacteria, while the liposomes (b, f) and PLGA nanoparticle cores without membrane coating (c, g) show negligible binding to bacteria. Independent experiments (n = 3) were performed with similar results.

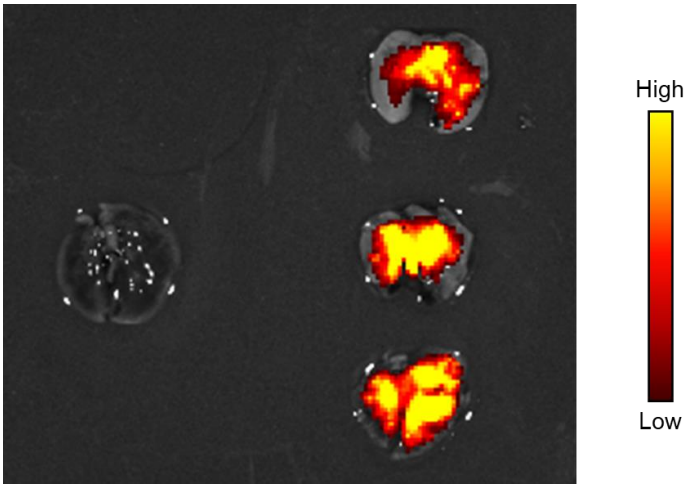

Supplementary Figure 18. Bacteria dispersion throughout the lung. Ex-vivo fluorescent image of the lungs at 1 hour after intratracheal inoculation of DiD-labeled *P. aeruginosa* (right). The control group (left) was treated with phosphate buffered saline (PBS).

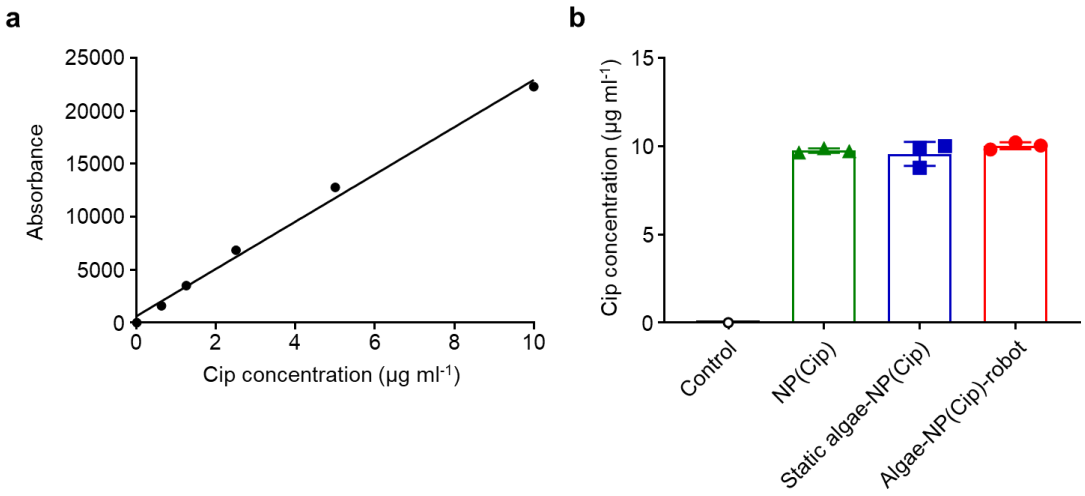

Supplementary Figure 19. Drug loading quantification. a, Calibration curve of ciprofloxacin. **b,** Quantification of ciprofloxacin amount for NP(Cip), static algae-NP(Cip), and algae-NP(Cip)-robot (n = 3; mean + s.d.).

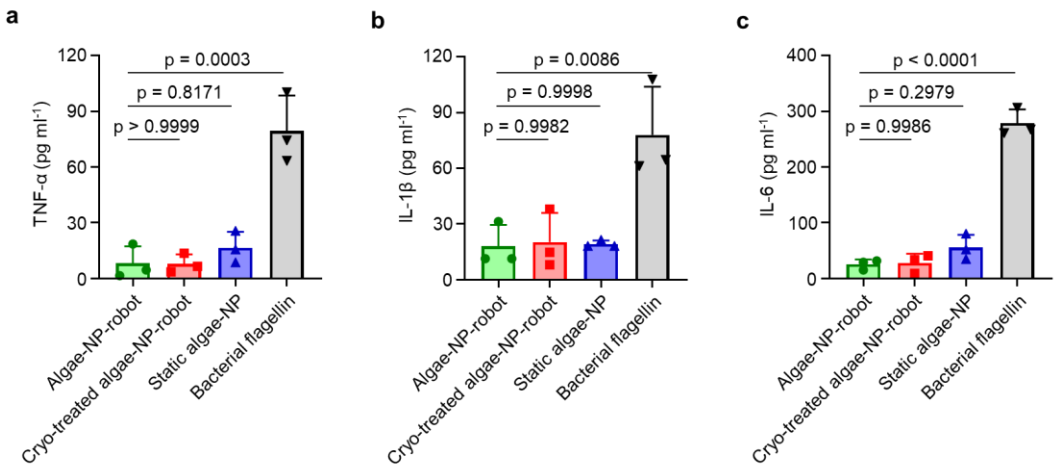

Supplementary Figure 20. In vitro algae-NP-robot induced cytokine production from J774 macrophages. a-c, Cytokines, including TNF-α (a), IL-1β (b), and IL-6 (c), induced by algae-NP-robot, cryo-treated algae-NP-robot, static algae-NP, or flagellin isolated from *Salmonella typhimurium* bacteria after 24 h incubation with J774 macrophage cells (n = 3; mean + s.d.). One-way ANOVA test.

Supplementary References

1. Sato, M., Murata, Y., Mizusawa, M., Iwahashi, H., Oka, S.-i. A Simple and rapid dual fluorescence viability assay for microalgae. Microbiol. Cult. Coll. 20, 53-59 (2004).

2. Zhang, Y. et al. A bioadhesive nanoparticle–hydrogel hybrid system for localized antimicrobial drug delivery. ACS Appl. Mater. Inter. 8, 18367 (2016).

3. Zhang, Q. et al. Neutrophil membrane-coated nanoparticles inhibit synovial inflammation and alleviate joint damage in inflammatory arthritis. Nat. Nanotechnol. 13, 1182 (2018).

Supplementary Table

Table S1. The composition of simulated lung fluid (SLF).

Ingredient	Concentration
DPPG	0.5 mg ml^{-1}
DPPC	4.8 mg ml^{-1}
Cholesterol	0.1 mg ml^{-1}
Albumin	8.8 mg ml^{-1}
IgG	2.6 mg ml^{-1}
Transferrin	1.5 mg ml^{-1}
Ascorbate	140 μM
Urate	95 μM
Glutathione	170 μM
Gentamicin	1 μl ml^{-1}
HBSS	77.5 μl ml^{-1}

Supplementary Movies

Supplementary Movie 1. Motion comparison of bare algae with algae-NP-robot in simulated lung fluid at body (37 °C) temperature at different operation times (0 min, 15 min, and 60 min).

Supplementary Movie 2. Representative 2 s tracking of algae-NP-robot in simulated lung fluid at body (37 °C) temperature at different operation times (0 min, 15 min, and 60 min).

Supplementary Movie 3. The motion of algae-NP-robot when co-cultured with macrophage.

Supplementary Movie 4. The motion of algae-NP-robot in simulated lung fluid at body temperature (37 °C) in the dark at various timepoints (12 h, 24 h, and 48 h).

Supplementary Movie 5. Random motion and phototaxis of algae-NP-robot under an external light source.